Numerical Analysis of the Shape of Bump Solutions in a Neuronal Model of Working Memory

Weronika Wojtak[1,2,a)], Flora Ferreira[1], Estela Bicho[1] and Wolfram Erlhagen[2]

[1]*Algoritmi Center, University of Minho, 4800-058 Guimarães, Portugal*
[2]*Center of Mathematics, University of Minho, 4800-058 Guimarães, Portugal*

[a)]Corresponding author: w.wojtak@dei.uminho.pt

Abstract. Neural field models, formalized by integro-differential equations, describe the large-scale spatio-temporal dynamics of neuronal populations [1]. They have been used in the past as a framework for modeling a wide range of brain functions, including multi-item working memory [2]. Neural field equations support spatially localized regions of high activity (or bumps) that are initially triggered by brief sensory inputs and subsequently become self-sustained by recurrent interactions within the neural population. We apply a special class of oscillatory coupling functions and analyze how the shape and spatial extension of multi-bump solutions change as the spatial ranges of excitation and inhibition within the field are varied [3]. More precisely, we use numerical continuation to find and follow solutions of neural field equations as the parameter controlling the distance between consecutive zeros of the coupling function is varied [4]. Important for a working memory application (e.g. [5]), we investigate how changes in this parameter affect the shape of bump solutions and therefore the maximum number of bumps that may exist in a given finite interval.

INTRODUCTION

Neural field models formalized by non-local integro-differential equations support a wide variety of dynamic behaviors observed in neural populations, such as waves [6], travelling pulses [7] and breathers [8]. For a recent review of neural field models and their solutions, we refer the reader to [9]. Of particular interest for modeling a working memory functionality are stationary pulse solutions (or bumps) that are initially triggered by brief sensory inputs and become self-sustained due to strong recurrent excitation and inhibition within the neural population [1]. In typical applications, the neural fields represent continuous input dimensions such as position, direction or color [3].

In order to represent the memory of a series of external stimuli, the field dynamics must support the existence of multiple regions of elevated persistent activity. Typically used connectivity functions of lateral inhibition type [1] do not generally support a stable pattern of two or more regions of high excitation. Motivated by periodic synaptic connectivity patterns observed in anatomical studies of prefrontal cortex [10] and visual cortex [11], we apply a class of periodically modulated coupling functions for which the existence of stable multi-bump solutions has been shown using analytical techniques [2, 3]. Here, we use complementary numerical tools to further investigate the pattern formation process in field models with oscillatory coupling. Specifically, we investigate how the shape and spatial extension of bump solutions change when the distance between consecutive zeros of the coupling function is systematically varied.

NEURAL FIELDS WITH OSCILLATORY COUPLINGS

The activity of a single layer of interconnected neurons along a one-dimensional finite domain $[-L, L]$ is governed by the equation:

$$\tau \frac{\partial u(x,t)}{\partial t} = -u(x,t) + \int_{-L}^{L} w(x-y) f(u(y,t) - h) \mathrm{d}y, \tag{1}$$

where τ defines the time scale of the field dynamics and $u(x,t)$ represents the activity at time t of a neuron at position x. The nonlinear function $f(u)$ represents the firing rate. Here we chose the Heaviside step function with threshold $h = 0$. The weight function $w(x-y)$ denotes the strength of connections between neurons separated by a distance y. It is defined as a periodically modulated connectivity function [2, 3]

$$w(x) = Ae^{-b|x|}(b\sin|\alpha x| + \cos(\alpha x)), \tag{2}$$

where A controls the amplitude, $b > 0$ the rate at which the oscillations decay with distance, and α the zero crossings of $w(x)$.

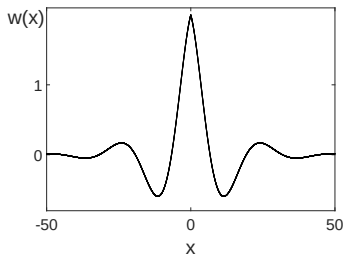

FIGURE 1. Coupling function with several positive zeros defined by Eq. 2 with $b = 0.1$, $A = 2$ and $\alpha = 0.3$.

RESULTS

Since solutions of Eq. 1 are invariant under translations [1], we are interested in finding steady states of Eq. 1 that are even, i.e., $u(x) = u(-x)$. We follow the approach in [4], expand these solutions $u(x)$ and the kernel $w(x)$ in Fourier series, substitute the two series in Eq. 1, and receive a system of ODEs. The steady states of these equations satisfy the following system of nonlinear equations

$$-u_j + w_j \int_{-L}^{L} \cos\left(\frac{j\pi y}{L}\right) f\left(\sum_{i=0}^{\infty} u_i(t)\cos\left(\frac{i\pi y}{L}\right) - h\right) \mathrm{d}y = 0, \tag{3}$$

for $j = 0, 1, \ldots, \infty$.
For the present numerical study, we use a finite Fourier series approximation with $M = 30$ terms. To find solutions of Eq. 3, determine their stability and follow them as parameter α of the connectivity function is varied, we apply numerical continuation. Specifically, we use the pseudo-arclength continuation method to carry out the numerical bifurcation analysis, treating α as a bifurcation parameter (for details of the technique see [4]). In order to ensure the existence of multi-bump solutions, we chose the specific threshold value $h = \int_0^{\frac{\pi}{\alpha}} w(x)\mathrm{d}x = W\left(\frac{\pi}{\alpha}\right)$ (for a mathematical analysis see [3]). In the next subsections, we report the results of following 1- and 2-bump solutions of Eq. 1 as the parameter α is changed.

1-bump solutions

The results for 1-bump solutions of system 3 are shown in Fig. 2. In the middle panel, the bump width a, defined as the interval of suprathreshold activity $h > 0$, is plotted as a function of α for three different threshold values. The left panel depicts the corresponding solutions of Eq. 1 at the points indicated by numbers in the middle panel. The right panel shows the widths of solutions for selected admissible values of α (see [3]), for which $h = W\left(\frac{\pi}{\alpha}\right)$. We note that for each value of α, a wider and a narrower bump coexist. Linear stability analysis shows that the wider bump is stable and the narrower bump is unstable [1]. The two solution branches annihilate in a saddle-node bifurcation with increasing α. This bifurcation structure has been previously observed with threshold h of the firing rate function (and fixed $w(x)$) [1] and b of the connectivity function [2] as bifurcation parameters.

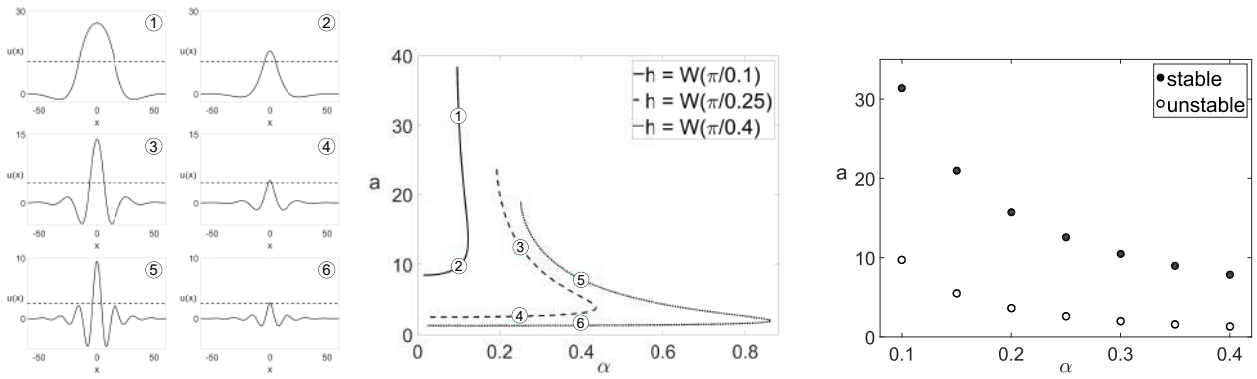

FIGURE 2. Analysis of 1-bump solutions of a neural field model. Left: Stable and unstable bumps corresponding to the numbers shown in the middle panel. Middle: The wide and narrow bumps are annihilated in a saddle-node bifurcation with increasing α and the width of the wider bump diverges to infinity with decreasing α. Right: Bump widths for admissible values of α for which $h = W\left(\frac{\pi}{\alpha}\right)$. Remaining parameters are $b = 0.1$ and $A = 2$.

2-bump solutions

We now solve system 3 with a bimodal initial condition to obtain 2-bump solutions with a minimum inter-peak distance d [3] and follow them as parameter α is changed. Similar to the case of a single bump, we find the coexistence of stable and unstable branches of 2-bump solutions for a range of admissible values of α for which the existence condition $h = W\left(\frac{\pi}{\alpha}\right)$ is satisfied. Note that with increasing α, not only the width a of each individual bump but also the peak distance d decreases.

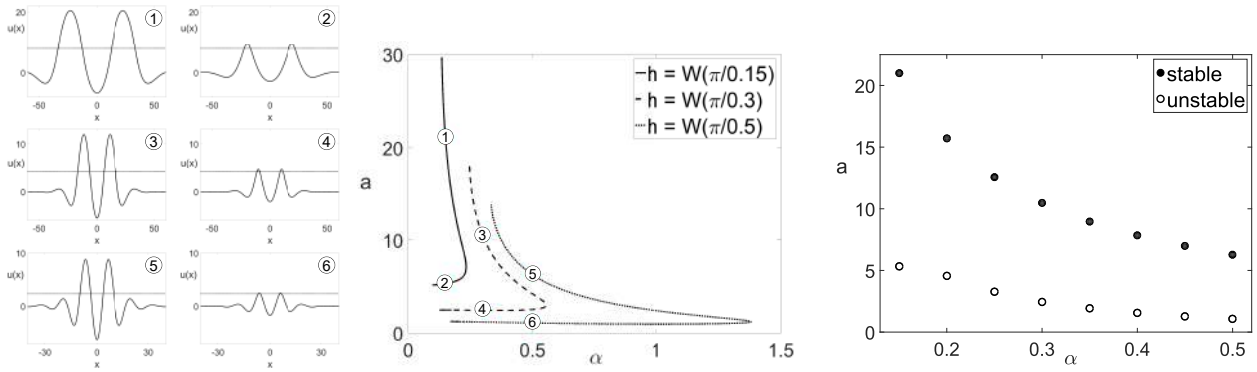

FIGURE 3. Analysis of 2-bump solutions of a neural field model. Left: Solution indicated by numbers in the middle panel. Middle: The wide and narrow 2-bumps are annihilated in a saddle-node bifurcation with increasing α and the width of the wider 2-bump diverges to infinity with decreasing α. Right: Widths of individual bumps for admissible values of α for which $h = W\left(\frac{\pi}{\alpha}\right)$. Remaining parameters are $b = 0.15$ and $A = 2$.

Multi-bump solutions

For a working memory application, an open research question is how many bumps may exist in a given finite interval of length 2L. Fig. 4 compares the summed width of all bumps of a stable N-bump solution as a function increasing α values for $N = 1, 2, 3$. For each α, the total excitation width is close to the predicted values when taking N times the width a of a single bump. Since also the minimum distance d between individual bumps decreases with increasing α, the maximum number of bumps, $N_{max} = \max_N(N\,a + (N-1)\,d < 2L)$, is predicted to increase with α. For the numerical example with $\alpha = 0.1$ the maximum numbers of bumps is 3.

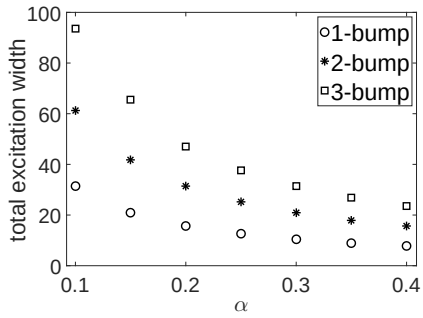

FIGURE 4. Summed width of all bumps of N-bump solutions as a function of α for $N = 1, 2, 3$.

DISCUSSION

We have applied the numerical continuation tools developed in [4] to perform a bifurcation analysis of a neural field model, treating parameter α, that determines the spatial ranges of excitation and inhibition within the field, as a bifurcation parameter. For 1- and 2-bump solutions, the generic picture consists of a branch of wider (stable) and a branch of narrower (unstable) bump solutions that are connected in a saddle-node bifurcation. Performing the full continuation analysis of N-bumps solutions for $N > 2$ turned out to be computationally quite heavy due to a necessarily fine spatial discretization of the interval. An alternative approach might be to use matrix-free Newton-Krylov solvers and perform numerical continuation of stationary solutions directly on the integral form of the equation [12]. Analysing N-bumps solutions with a more efficient continuation scheme may allow investigating whether branches of localized solutions exhibit snaking-type behaviour in terms of parameter α, a behaviour previously observed in neural field models for other parameters [13]. It would be also interesting to perform a multi-parameter analysis to describe the exact regions for which localized solutions exist in terms of all three parameters of the oscillatory kernel.

ACKNOWLEDGMENTS

The work received financial support from FCT through the PhD fellowship PD/BD/128183/2016.

REFERENCES

[1] S. Amari, Biological Cybernetics **27**, 77–87 (1977).
[2] C. R. Laing, W. C. Troy, B. Gutkin, and G. B. Ermentrout, SIAM Journal on Applied Mathematics **63**, 62–97 (2002).
[3] F. Ferreira, W. Erlhagen, and E. Bicho, Physica D: Nonlinear Phenomena **326**, 32–51 (2016).
[4] C. R. Laing, The Journal of Mathematical Neuroscience **4**, p. 13 (2014).
[5] E. Sousa, W. Erlhagen, F. Ferreira, and E. Bicho, Neural Networks **72**, 123–139 (2015).
[6] G. B. Ermentrout and J. B. McLeod, Proceedings of the Royal Society of Edinburgh Section A: Mathematics **123**, 461–478 (1993).
[7] D. J. Pinto and G. B. Ermentrout, SIAM Journal on Applied Mathematics **62**, 206–225 (2001).
[8] S. E. Folias and P. C. Bressloff, Physical review letters **95**, 208–107 (2005).
[9] S. Coombes, Biological Cybernetics **93**, 91–108 (2005).
[10] J. B. Levitt, D. A. Lewis, T. Yoshioka, and J. S. Lund, The Journal of Comparative Neurology **338**, 360–376 (1993).
[11] A. Angelucci, J. B. Levitt, E. J. S. Walton, J.-M. Hupé, J. Bullier, and J. S. Lund, Journal of Neuroscience **22**, 8633–8646 (2002).
[12] J. Rankin, D. Avitabile, J. Baladron, G. Faye, and D. J. Lloyd, SIAM Journal on Scientific Computing **36**, B70–B93 (2014).
[13] D. Avitabile and H. Schmidt, Physica D: Nonlinear Phenomena **294**, 24–36 (2015).